

Diffusion and conduction in a salt-free colloidal suspension via molecular dynamics simulations

Sorin Bastea*

Lawrence Livermore National Laboratory, 7000 East Ave., Livermore, CA 94550

Molecular dynamics (MD) simulations are used to determine the diffusion coefficients, electrophoretic mobilities and electrical conductivity of a charged colloidal suspension in the salt-free regime as a function of the colloid charge. The behavior of the colloidal particles' diffusion constant can be well understood in terms of two coupled effects: counterion 'condensation' and slowdown due to the relaxation effect. We find that the conductivity exhibits a maximum which approximately separates the regimes of counterion-dominated and colloid-dominated conduction. We analyze the electrophoretic mobilities and the conductivity in terms of commonly employed assumptions about the role of "free" and "condensed" counterions, and discuss different interpretations of this approach.

Charged colloidal suspensions exhibit a wide range of interesting equilibrium as well as electrokinetic behaviors. On the equilibrium side these include charge renormalization due to strong counterion screening [1–3], large Coulombic effects in sedimentation profiles [4], highly tunable phase transitions [5, 6], solvation charge asymmetry effects [7], *et caetera*. The dynamic behavior may be even richer due to the coupling of hydrodynamic and electrostatic interactions [8–11]. The motion of charged, mesoscopically-sized particles such as colloids or polyelectrolytes in applied electric fields, generally referred to as electrophoresis, is relevant to numerous applications, from the detection of elementary charges [12] to molecular biology [13] and nanofluidics [14]. As a result, the interest in elucidating fundamental aspects of this phenomenon remains high [15, 16], with computer simulations playing a significant role [17–19]. Although the focus of such studies is often only the electrophoretic mobility [15, 18], the behavior of the self-diffusion coefficient and electrical conductivity are also important features of these systems [20, 21]. Electrophoretic mobility and electrical conductivity measurements are in fact routine characterization tools for the charge and number density of colloidal particles [4, 21], while the determination of the diffusion constant is commonly used to obtain information on their size [22]. Since these are the major parameters determining the stability, structure and phase behavior of colloidal suspensions [5, 23], unraveling the mechanisms controlling charge and diffusive transport and their exact relation to colloidal charge, size and density is crucial for understanding the properties of charged suspensions and how to potentially control them. Numerical simulations are an important avenue for elucidating such connections and new methods based on coupling the equations of motion of the colloidal particles with hydrodynamics equations for the solvent have recently proved valuable for studying the electrophoretic mobility [18, 19, 24], while Brownian dynamics simulations have yielded all transport coefficients [25]. Molecular dynamics (MD) simulations are a complementary tool for such studies and can directly capture the complex interplay of short and long range interactions as well as solvent structure and hydrodynamics which are relevant for transport processes in colloids, but have been previously limited to single colloidal particle systems [17, 26, 27]. In this letter we present MD simulation results for the electrical conductivity, self-diffusion coefficients and electrical mobilities of a charged colloidal suspension under no-salt conditions. Such suspensions can provide substantial insight for example into surface charge regulation effects [28], and they have recently began to be studied more systematically, with results now available for both structural [29] and electrokinetic properties [26].

The system considered here contains solvent particles, colloidal particles with charge $-Ze$ and counterions of opposite unit charge, i.e. it is a salt-less suspension. The inter-particle potentials consist of short range and Coulomb contributions. The short range interactions are based on the inverse-12, 'soft-sphere' potential,

$$u(r) = \epsilon \left(\frac{d_0}{r} \right)^{12} \quad (1)$$

, which we truncate and shift at $r/d_0 = 2$. (We also define $u(r) = \infty$ for $r < 0$.) They are:

$$u_{CC}(r) = u(r - 2R_C) \quad (2a)$$

$$u_{Cc}(r) = u_{Cs}(r) = u(r - R_C) \quad (2b)$$

$$u_{cc}(r) = u_{ss}(r) = u_{cs}(r) = u(r) \quad (2c)$$

, where C , c and s denote the colloidal particles, counterions and solvent particles, respectively; R_C is an impenetrable colloidal particle core radius. Such potentials have been employed before to model neutral suspensions [30, 31]. For temperatures $k_B T \simeq \epsilon$ the effective diameters corresponding to these interactions are well approximated by

$d_\gamma = d_{cs} = d_0$, $d_C = 2R_C + d_0$, and $d_{C\gamma} = R_C + d_0$, and satisfy additivity, $d_{C\gamma} = (d_C + d_\gamma)/2$; $\gamma = c, s$. The Coulomb interactions are given by

$$v_{\alpha\beta}(r) = \frac{1}{4\pi\epsilon_0\epsilon_r} \frac{q_\alpha q_\beta}{r} \quad (3)$$

where $\alpha, \beta = c, C$. Thus, while the solvent size granularity is explicitly accounted for at the microscopic level by the short range interactions, the (relative) dielectric constant ϵ_r , as is usually the case [23, 32], is not. It would be difficult to perform large scale simulations with solvent particles carrying explicit dipoles, and we do not expect that they would change the results reported here.

We focused on suspensions with colloid 'volume fraction' $\phi_C = \pi n_C d_C^3/6 = 0.1$, solvent plus counterions 'volume fraction' $\phi_0 = \pi(n_c + n_s)d_0^3/6 = 0.35$, and with a colloid-solvent 'diameter' ratio $d_C/d_0 = 10$; n_δ ($\delta = C, c, s$) are the number densities and satisfy $n_c = Zn_C$ due to charge conservation. We performed MD simulations of this system (which may be viewed as a model nanocolloidal suspension) in the microcanonical (NVE) ensemble for 8 different values of the colloidal charge Z : 0, 10, 20, 30, 40, 50, 70, 100 at an average temperature $k_B T = \epsilon$. If we introduce the Bjerrum length $\lambda_B = e^2/4\pi\epsilon_0\epsilon_r k_B T$ and Debye screening distance associated with counterions only, $\lambda_D = (4\pi\lambda_B n_c)^{-1/2}$, the simulations correspond to $\lambda_B/d_0 = 2.32$, while λ_D/d_0 varied between 4.23 for the $Z = 10$ simulations and 1.34 for the $Z = 100$ ones. The particle masses were $m_s = m_c = m_0$ and $m_C/m_0 = 1000$. All simulations were carried out with $N_C = 50$ and $N_s + N_c = 175000$ in a box with periodic boundaries. The Coulomb interactions were handled using the Ewald summation technique with conducting boundary conditions. The time, electrical conductivity and electrical mobility units are $t_0 = d_0(m_0/\epsilon)^{1/2}$, $\sigma_0 = 10^{-4} \times e^2 t_0/m_0 d_0^3$ and $\mu_0 = e t_0/m_0$, respectively.

After equilibration the simulations were run for $\simeq 5 \times 10^5$ time steps ($\simeq 4000 t_0$), accumulating structural as well as dynamic information necessary for the calculation of self-diffusion, electrical conductivity and electrophoretic mobilities. The self-diffusion coefficients D_δ , $\delta = C, c, s$ were determined using the velocity autocorrelation relation:

$$D_\delta = \lim_{t \rightarrow \infty} \frac{1}{3} \int_0^t \langle \mathbf{v}_\delta(0) \cdot \mathbf{v}_\delta(\tau) \rangle d\tau \quad (4)$$

with no tail corrections. The conductivity calculation was done by integrating the charge current autocorrelation,

$$\sigma = \lim_{t \rightarrow \infty} \frac{1}{3V k_B T} \int_0^t \langle \mathbf{j}^q(0) \cdot \mathbf{j}^q(\tau) \rangle d\tau \quad (5a)$$

$$\mathbf{j}^q(t) = \sum_i^N q_i \mathbf{v}_i(t) = e[\mathbf{j}_c^d(t) - Z\mathbf{j}_C^d(t)] \quad (5b)$$

$$\mathbf{j}_\delta^d(t) = \sum_i^{N_\delta} \mathbf{v}_{i\delta}(t) \quad (5c)$$

The electrophoretic mobilities of the colloidal particles and counterions can also be calculated in the Green-Kubo framework by integrating the charge - diffusion currents correlations [27]:

$$\mu_\delta^E = \lim_{t \rightarrow \infty} \frac{1}{3N_\delta k_B T} \int_0^t \langle \mathbf{j}^q(0) \cdot \mathbf{j}_\delta^d(\tau) \rangle d\tau \quad (6)$$

Thus σ can be written in terms of the mobilities in its canonical form:

$$\sigma = e(n_c \mu_c^E - n_C Z \mu_C^E) \quad (7)$$

It is worth noting that μ_C^E is the electrical mobility in suspension and not for an isolated particle, as often studied theoretically and measured under very dilute conditions.

The colloid-counterion pair correlation functions - Fig. 1 - show strong counterion stratification at the surface of the colloidal particles and the formation of what is typically designated as the Stern layer [23], with a thickness of roughly one counterion diameter. This surface 'condensation' effect and the associated chemical equilibrium between 'condensed' and 'free' counterions leads to colloid-colloid interactions corresponding to a renormalized or effective colloid charge Z_{eff} , which saturates at large Z [1, 2]. We test this scenario by defining Z_{eff} in the natural way, as the charge contained on the average in a sphere centered on a colloidal particle and extending up to the first minimum of $g_{Cc}(r)$, i.e. inside the outer boundary of the Stern layer. Other, related definitions are also possible [33], but they yield similar outcomes. The result is plotted in Fig. 1 (inset) and shows that Z_{eff} so defined exhibits the predicted

saturation behavior in the range of 'bare' charges Z covered in these simulations. Being defined in terms of $g_{Cc}(r)$, Z_{eff} includes the effect of the counterions size. We note that since the system is salt-free and all counterions are identical subtle phenomena associated with size asymmetry between the anions and cations such as charge reversal and charge amplification [34] are not expected here. It would be very interesting to study the influence of such effects on the electrokinetic properties of charged colloids, since size-asymmetry is common in real situations. We should also remark that for such systems the definition of Z_{eff} would likely need to be revised, perhaps by assuming that the charge layer extends up to the first minimum of the total number density of ions; this issue requires however further careful study.

The self-diffusion coefficients of the colloidal particles and counterions - Fig. 2 (see also top inset of Fig. 3), are both decreasing functions of Z . Their behavior can likely be understood by extending to charged colloidal systems arguments usually employed for the self-diffusion coefficients of electrolyte solutions. The classic analysis due to Onsager [35] singles out the most important contribution to self-diffusion to be the relaxation effect, i.e. the drag exercised on a moving ion by its lagging, distorted charge atmosphere. This direct, phenomenological treatment is particularly suitable for the colloidal particles, which are primarily screened by the small counterions. In this case the ionic atmosphere subject to relaxation should reasonably be expected to consist only of the counterions beyond the tightly "bound" Stern layer, so an analysis in terms of the effective charge Z_{eff} is likely appropriate; we outline it below following the ideas in [35]. The screening atmosphere of a charged colloidal particle moving with velocity v will lag behind a distance ζ equal with the one traveled by the particle in the time τ that the atmosphere (a charge shell of typical size λ_D) needs to equilibrate through diffusive redistribution of the screening counterions: $\zeta = v\tau$, where $\tau \propto \lambda_D^2/D_c$ and $D_c = k_B T/\xi$ (Einstein relation for counterions), with friction coefficient $\xi \propto \eta d_c$ (Stokes relation with viscosity η). This lag or distortion will result in a retarding force between the charged particle and its screening atmosphere, $F_r \propto \zeta Z_{eff}^2 e^2 / \lambda_D^3 \epsilon_r$. Since the Stokes drag on the colloidal particle is $F_s \propto \eta d_C v$, the total drag force will be

$$F_{total} = F_s + F_r \propto \eta d_C v [1 + f \lambda_B (d_c/d_C) Z_{eff}^2 / \lambda_D] \quad (8)$$

, where f is a numerical factor. This corresponds to an effective friction coefficient

$$\xi t \propto \eta d_C [1 + f (d_c/d_C) Z_{eff}^2 \lambda_B / \lambda_D] \quad (9)$$

, which yields, according to the Einstein relation, the self-diffusion coefficient of the charged colloidal particles:

$$D_C = \frac{D_0}{1 + f \frac{d_c}{d_C} \frac{\lambda_B}{\lambda_D} Z_{eff}^2} \quad (10)$$

The Onsager relation for diffusion in electrolytes with equally sized anions and cations (whose derivation requires additional assumptions and is similar but not identical with Eq. 10) also determines the factor f , e.g. $f \simeq 0.1$ for the charge symmetric case [35]. For the present highly asymmetric charged colloidal system we test the relaxation effect prediction by assuming f to be a free parameter. The comparison with the MD results, shown in Fig. 2 (inset) with $f \simeq 0.022$, indicates that the concept of renormalized charge is suitable for describing the self-diffusive motion of charged colloids in conjunction with the relaxation effect. This may provide a convenient avenue for estimating the self-diffusion coefficients of such colloids over a wide range of charged states. We note that the relative diffusion constant D_C/D_0 satisfies the scaling ansatz introduced in [26] for colloidal suspensions in the low-salt regime. Its behavior however is different from the standard Einstein relation usually assumed for charged colloids [22].

Electrical conductivity (σ) measurements are an important means for characterizing the properties of charged suspensions [4, 21]. The MD simulations reveal that σ exhibits a maximum as a function of the 'bare' charge Z - Fig. 3. Such a behavior has been previously observed for the electrophoretic mobility of short polyelectrolyte chains [10], as well as in simulations of a single charged colloidal particle at low volume fraction [27, 36]. In the present simulations the behavior of the counterion and colloid electrophoretic mobilities - Fig. 3 (bottom - inset), indicates that the conductivity maximum roughly separates the regimes of counterion-dominated and colloid-dominated conduction. Theories for electrical conduction in classical charged systems such as electrolytes have a long history [37, 38] but their generalization to charged colloids is difficult. Common interpretations of electrical conduction rely on the counterion condensation effect and the assumption of "free" and "condensed" counterion populations that contribute differently to charge transport [40]. We examine below to what extent this picture can be reconciled with the observed behavior.

Using charge conservation the conductivity equation Eq. 7 can be written as

$$\sigma = en_C Z (\mu_c^E + \mu_C^E) \quad (11)$$

, where for simplicity we denote $(-\mu_C^E)$ by μ_C^E , a positive quantity. On the other hand the assumption of “free” and “condensed” counterions is usually used to write the conductivity as

$$\sigma = en_C Z_{eff}^* (\mu_{cf}^E + \mu_C^E) \quad (12)$$

, where now only $n_C Z_{eff}^*$ counterions are assumed to be “free”, with mobility μ_{cf}^E . This equation holds exactly if $(Z - Z_{eff}^*)$ counterions are essentially “attached” to each colloidal particle, and therefore have the exact same mobility with it. In reality however the “condensed” and “free” counterions are not separated populations, and the physical, commonly accepted picture is one of chemical equilibrium between them [1]. The present simulations are consistent with this picture, as they show a continuous exchange between the “condensed” and “free” counterions as previously defined based on $g_{Cc}(r)$. We estimate for example that the average exchange rate (per particle) is of the order $3.0 \times 10^{-2} t_0^{-1}$. Thus, as opposed to μ_c^E and μ_C^E , which are given by Eq. 6, the “free” ions mobility μ_{cf}^E is not a very well defined quantity. Moreover, even if some reasonable interpretation for μ_{cf}^E is adopted, e.g. the single particle, high dilution mobility, Z_{eff}^* can only be understood as being defined by Eqs. 11 and 12. Thus, there is no *a priori* reason why Z_{eff}^* should be exactly identified with Z_{eff} , although there is a reasonable expectation that they should behave similarly. We also note that simple assumptions about the relation between μ_c^E and μ_{cf}^E such as $\mu_c^E = (Z_{eff}^*/Z) \mu_{cf}^E$ are not compatible with Eq. 11 unless μ_C^E is zero, or at least $\mu_C^E \ll \mu_c^E$.

We now consider some possible interpretations of the simulation results, using the Nernst-Einstein relation [39], which connects the self-diffusion constants to the mobilities and the electrical conductivity. The simplest application of this relation suggests that the conductivity, Eq. 11, should be written as

$$\sigma = e^2 n_C Z (D_c + Z D_C) / k_B T \quad (13)$$

, with mobilities

$$\mu_C^E = e Z D_C / k_B T \quad (14a)$$

$$\mu_c^E = e D_c / k_B T \quad (14b)$$

Not surprisingly this is not a good approximation as it deviates rapidly at low Z from the simulation results, and predicts a monotonously increasing conductivity - see Fig. 3 (bottom). The main reason for the large discrepancy is likely the implicit neglect in the above relation of the correlations between particles and counterions, which is not consistent with the existence of a tightly “bound” counterions layer. Such deviations from ideal behavior have also been noted in Brownian dynamics simulations of charged suspensions [25].

The Nernst-Einstein relation can also be written starting from Eq. 12, as

$$\sigma = e^2 n_C Z_{eff}^* (D_{cf} + Z_{eff}^* D_C) / k_B T \quad (15)$$

, with mobilities

$$\mu_C^E = e Z_{eff}^* D_C / k_B T \quad (16a)$$

$$\mu_{cf}^E = e D_{cf} / k_B T \quad (16b)$$

This however requires some interpretation on the meaning of D_{cf} , the diffusion constant of “free” counterions. We assume here that $D_c(Z=0)$ is a reasonable measure for D_{cf} , and identify it with the diffusion constant of the solvent, D_s , since the counterions and solvent particles are identical in the limit $Z=0$; this quantity is independent of Z , and in fact $D_c(Z=10)$ is already essentially identical with D_s . This assumption is in line with usual conductivity modeling based on Eq. 12 [21, 40]. We then identify Z_{eff}^* with Z_{eff} , and plot the results in Fig. 3. This relation underestimates the conductivity results, and overestimates the mobility of the colloidal particles. Moreover, the qualitative behavior of these quantities is different than the simulations, as they both exhibit plateaus at high Z . We note that the observed decrease in mobility at high Z is in agreement with previous simulations, for example those reported in [36].

To make further progress we adopt therefore the following ansatz: we assume that the mobilities of the counterions and colloids μ_c and μ_C are proportional with their respective diffusion constants D_c and D_C , and that the conductivity relation reduces to the original Nernst-Einstein form Eq. 13 when $Z_{eff} \rightarrow Z$. The simplest such form is

$$\sigma = e^2 n_C Z_{eff}^* (D_c + Z_{eff}^* D_C) / k_B T \quad (17)$$

, with mobilities

$$\mu_C^E = e(Z_{eff}^*/Z)(D_C/k_B T) \quad (18a)$$

$$\mu_c^E = e(Z_{eff}^*/Z)(D_c/k_B T) \quad (18b)$$

The μ_c^E equation is consistent with the idea that only a fraction of the counterions, Z_{eff}^*/Z , participate on average in electrical conduction as “free” charges. The conductivity equation Eq. 17 predicts a maximum, but its value is smaller than that observed in the simulations if Z_{eff}^* is identified with Z_{eff} . To get better agreement we adopt a simple rescaling, $Z_{eff}^* = 1.4Z_{eff}$. Incidentally this scaling factor is similar with the one previously determined by comparing effective colloidal charges from structural and conductivity measurements [21]. However, while such a factor may signal a difference between static and dynamic effective charges (see also below), we do not regard this particular value as carrying fundamental significance. We plot the results in Fig. 4. The agreement is good for the counterions mobility and at least qualitative for the conductivity. On the other hand the μ_C^E relation appears to hold well only at high Z . Nevertheless, it is worth studying further the validity of Eq. 18a in the effective charge saturation regime (high Z), since there it would imply $(\mu_C^E)^{-1} \propto Z$, which may perhaps be employed for a direct determination of the charge [12].

The above discussion highlights the inherent limitations of the effective charge representation and “free” and “condensed” counterions picture in the context of electrical conduction and electrophoretic mobilities. To the extent that it is appropriate to regard Eq. 18b as implicitly defining a dynamic effective charge, it also supports the notion that static and dynamic definitions of the effective charge lead to different results [17, 21]. To gain further insight into why more counterions may dynamically behave as “free”, as suggested by the above effective charge rescaling, we consider the pair correlation function between colloidal particles and counterions + solvent particles - $g_{Cc+s}(r)$ - Fig. 4, which exhibits strong layering at short distances and on intermediate length scales converges to $1/(1 - \phi_C)$, corresponding to a higher apparent interstitial fluid density. We define the position (r_b) right after the first peak of $g_{Cc+s}(r)$ where this density is reached as a boundary fluid layer, and calculate the effective charge contained in this shell. We also determine the charge shell boundary r_σ corresponding to Z_{eff}^* , and find that it agrees well with r_b , particularly at the highest Z 's - Fig. 4 (inset). Both are approximately half a counterion diameter smaller than r_0 , the first minimum of $g_{Cc}(r)$, which defines the Stern layer and Z_{eff} . This suggests that at high Z , Z_{eff}^* may correspond to the boundary fluid layer at the surface of the colloidal particles, which is thinner than the Stern layer. Of course such a connection is at this point somewhat speculative and would certainly benefit from additional study, for example by analyzing at the MD level the velocity correlations between the colloidal particles and the “condensed” counterions under an applied electric field [17, 36].

In sum, MD simulations of a charged colloidal suspension in the salt-free regime yield the diffusion constants, mobilities and conductivity, and help clarify the interplay between charge saturation and slowdown due to the relaxation effect in the diffusive motion of colloidal particles. The system exhibits an electrical conductivity maximum as a function of the colloid charge, which roughly separates the regimes of counterion-dominated and colloid-dominated conduction. We analyze the electrophoretic mobilities and conductivity using commonly employed assumptions about the role of the effective charge, “free” and “condensed” counterions, and discuss different interpretations and some of the limitations of this approach. We also find, in agreement with previous observations, that in the effective charge saturation regime the effective transported charge appears to be larger than the one determined by the Stern layer, and speculate that it corresponds to the boundary fluid layer at the surface of the colloidal particles. Future simulations such as the one presented here may help further elucidate this issue. They should also be useful for studying the dependence of the diffusion constants, mobilities and conductivity on the colloidal volume fraction, which has only recently been addressed using many particle systems [18]. Finally, it may be interesting to study electrokinetic effects in charged colloidal dispersions with lower solvent dielectric constants, where clustering effects may play an important role [41].

This work was performed under the auspices of the U. S. Department of Energy by Lawrence Livermore National Laboratory under Contract DE-AC52-07NA27344.

* Electronic address: sbastea@llnl.gov

- [1] S. Alexander, P.M. Chaikin, P. Grant, G.J. Morales, P. Pincus, J. Chem. Phys. **80**, 5776 (1984).
- [2] Y. Levin, M.C. Barbosa, M.N. Tamashiro, Europhys. Lett. **41**, 123 (1998).
- [3] A. Torres, G. Téllez, R. van Roij, J. Chem. Phys. **128**, 154906 (2008).
- [4] M. Raşa, A.P. Philipse, Nature **429**, 857 (2004).

- [5] B. Zoetekouw, R. van Roij, Phys. Rev. Lett. **97**, 258302 (2006).
- [6] H. Guo, T. Narayanan, M. Sztuchi, P. Schall, G. H. Wegdam, Phys. Rev. Lett. **100**, 188303 (2008).
- [7] W. Kung, P. González-Mozuelos, M. Olvera de la Cruz, Soft Matter **6**, 331 (2010).
- [8] D.O. Riese, G.H. Wegdam, W.L. Vos, R. Sprik, D. Fenistein, J.H.H. Bongaerts, G. Grübel, Phys. Rev. Lett. **85**, 5460 (2000).
- [9] L. Joly, C. Ybert, E. Trizac, L. Bocquet, Phys. Rev. Lett. **93**, 257805 (2004).
- [10] K. Grass, U. Böhme, U. Scheler, H. Cottet, C. Holm, Phys. Rev. Lett. **100**, 096104 (2008).
- [11] A. Würger, Phys. Rev. Lett. **101**, 108302 (2008).
- [12] F. Strubbe, F. Beunis, K. Neyts, Phys. Rev. Lett. **100**, 218301 (2008).
- [13] J.-L. Viovy, Rev. Mod. Phys. **72**, 813 (2000).
- [14] R.B. Schoch, J. Han, P. Renaud, Rev. Mod. Phys. **80**, 839 (2008).
- [15] A.A. Shugai, S.L. Carnie, D.Y.C. Chan, J.L. Anderson, J. Colloid Interface Sci. **191**, 357 (1997).
- [16] J. Ennis, L.R. White, J. Colloid Interface Sci. **185**, 157 (1997).
- [17] V. Lobaskin, B. Dünweg, C. Holm, J. Phys. Condens. Matter **16**, S4063 (2004).
- [18] K. Kim, Y. Nakayama, R. Yamamoto, Phys. Rev. Lett. **96**, 208302 (2006).
- [19] T. Araki, H. Tanaka, Europhys. Lett. **82**, 18004 (2008).
- [20] D. Ertas, Phys. Rev. Lett. **80**, 1548 (1998).
- [21] P. Wette, H.J. Schöpe, T. Palberg, J. Chem. Phys. **116**, 10981 (2002).
- [22] F. Strubbe, F. Beunis, K. Neyts, J. Colloid and Interface Sci. **301**, 302 (2006).
- [23] J.-P. Hansen, H. Löwen, Annu. Rev. Phys. Chem. **51**, 209 (2000).
- [24] A. Chatterji, J. Horbach, J. Chem. Phys. **122**, 184903 (2005).
- [25] V. Dahirel, M. Jardat, J.F. Dufrêche, P. Turq, J. Chem. Phys. **131**, 234105 (2009).
- [26] V. Lobaskin, B. Dünweg, M. Medebach, T. Palberg, C. Holm, Phys. Rev. Lett. **98**, 176105 (2007).
- [27] B. Dünweg, V. Lobaskin, K. Seethalakshmy-Hariharan, C. Holm, J. Phys. Condens. Matter **20**, 404214 (2008).
- [28] R. Karnik, R. Fan, M. Yue, D. Li, P. Yang, A. Majundar, Nano. Lett. **5**, 943 (2005).
- [29] L.F. Rojas-Ochoa, R. Castaneda-Priego, V. Lobaskin, A. Stradner, F. Scheffold, P. Schurtenberger, Phys. Rev. Lett. **100**, 178304 (2008).
- [30] S. Bastea, Phys. Rev. Lett. **96**, 028305 (2006).
- [31] S. Bastea, Phys. Rev. E **75**, 031201 (2007).
- [32] T.S. Lo, B. Khusid, J. Koplik, Phys. Rev. Lett. **100**, 128301 (2008).
- [33] L. Belloni, Colloids Surf. A **140**, 227 (1998).
- [34] G.I. Guerrero-García, E. González-Tovar, M. Olvera de la Cruz, Soft Matter **6**, 2056 (2010).
- [35] L. Onsager, Ann. N. Y. Acad. Sci. **46**, 241 (1945).
- [36] A. Chatterji, J. Horbach, J. Chem. Phys. **126**, 064907 (2007).
- [37] R.M. Fuoss, L. Onsager, Proc. N. A. S. **41**, 274 (1955).
- [38] T.J. Murphy, E.G.D. Cohen, J. Chem. Phys. **53**, 2173 (1970).
- [39] See, e.g., J.-P. Hansen, I.R. McDonald, *Theory of Simple Liquids*, 2nd edition, (Academic Press, London, 1986).
- [40] M. Medebach, R.C. Jordán, H. Reiber, H.-J. Schöpe, R. Biehl, M. Evers, D. Hessinger, J. Olah, T. Palberg, E. Schönberger, P. Wette, J. Chem. Phys. **123**, 104903 (2005).
- [41] See, e.g., S. Bastea, Phys. Rev. E **66**, 020801(R) (2002) and references therein.

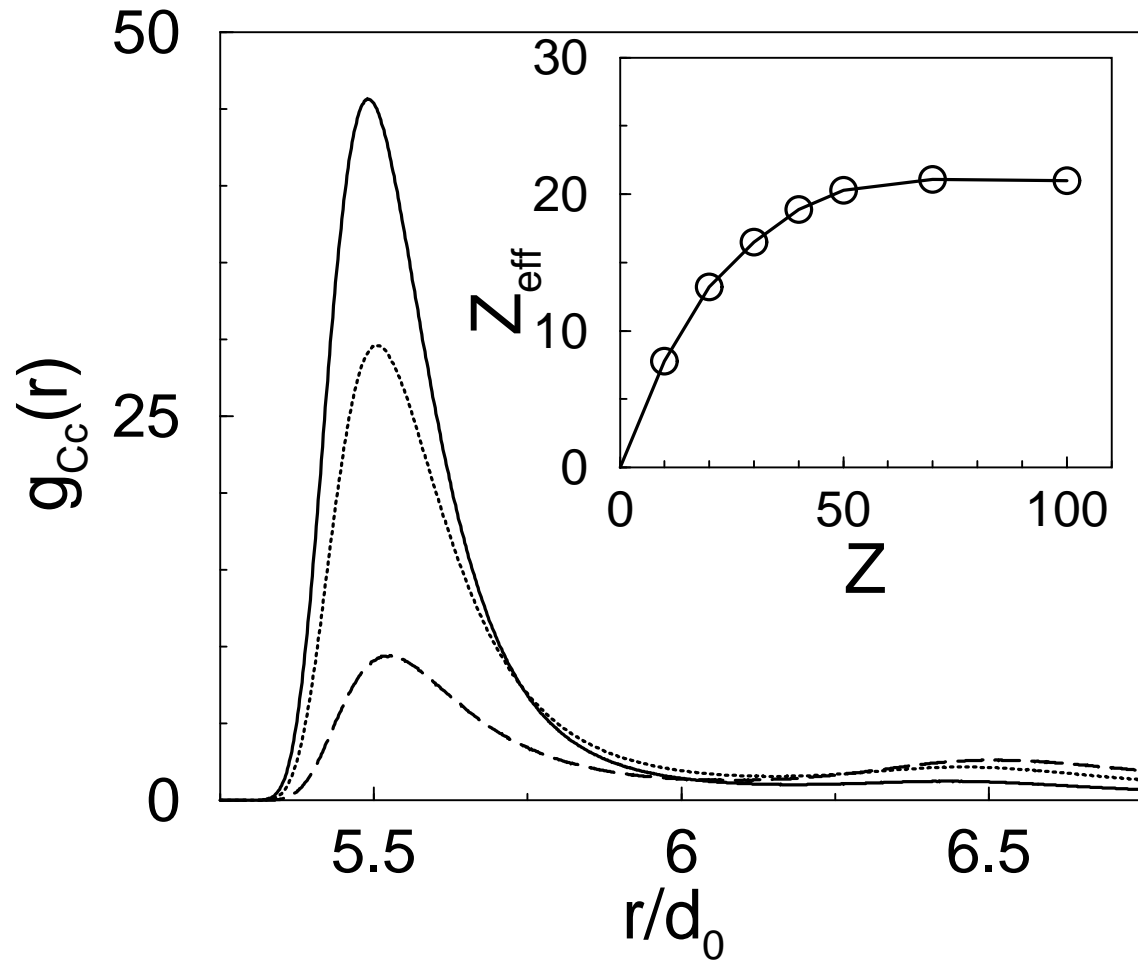


FIG. 1: Colloid-counterion pair correlation function for $Z = 10$ (dashed line), 50 (dotted line), 100 (solid line). Inset: effective colloidal particle charge Z_{eff} as a function of the 'bare' charge Z .

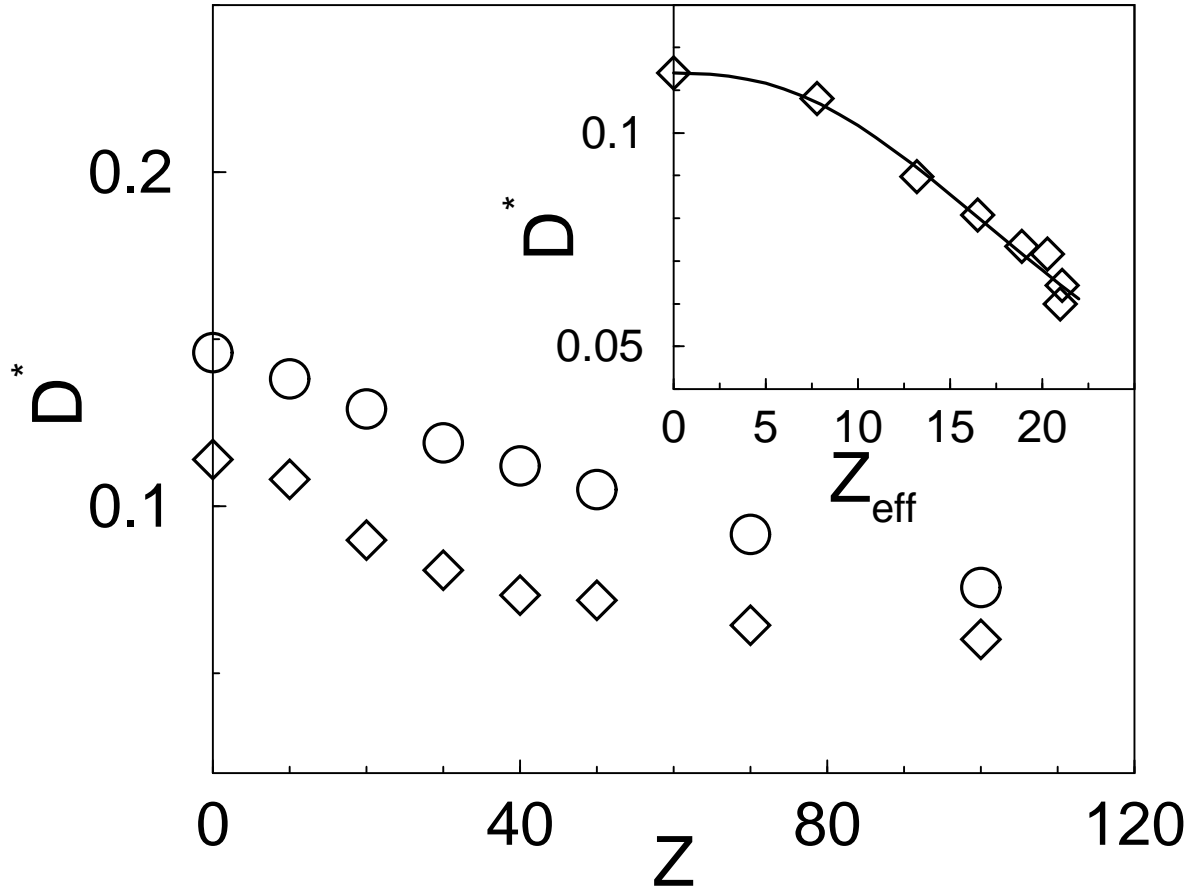


FIG. 2: Self-diffusion coefficients of counterions (circles) and colloidal particles (diamonds) as a function of colloid charge Z ; $D^* = D_\alpha d_\alpha / D_0 d_0$, $D_0 = d_0^2 / t_0$, $\alpha = c, C$. Inset: Colloidal particle self-diffusion coefficient as a function of the effective charge Z_{eff} (symbols) and relaxation effect relation - Eq. 10 (solid line).

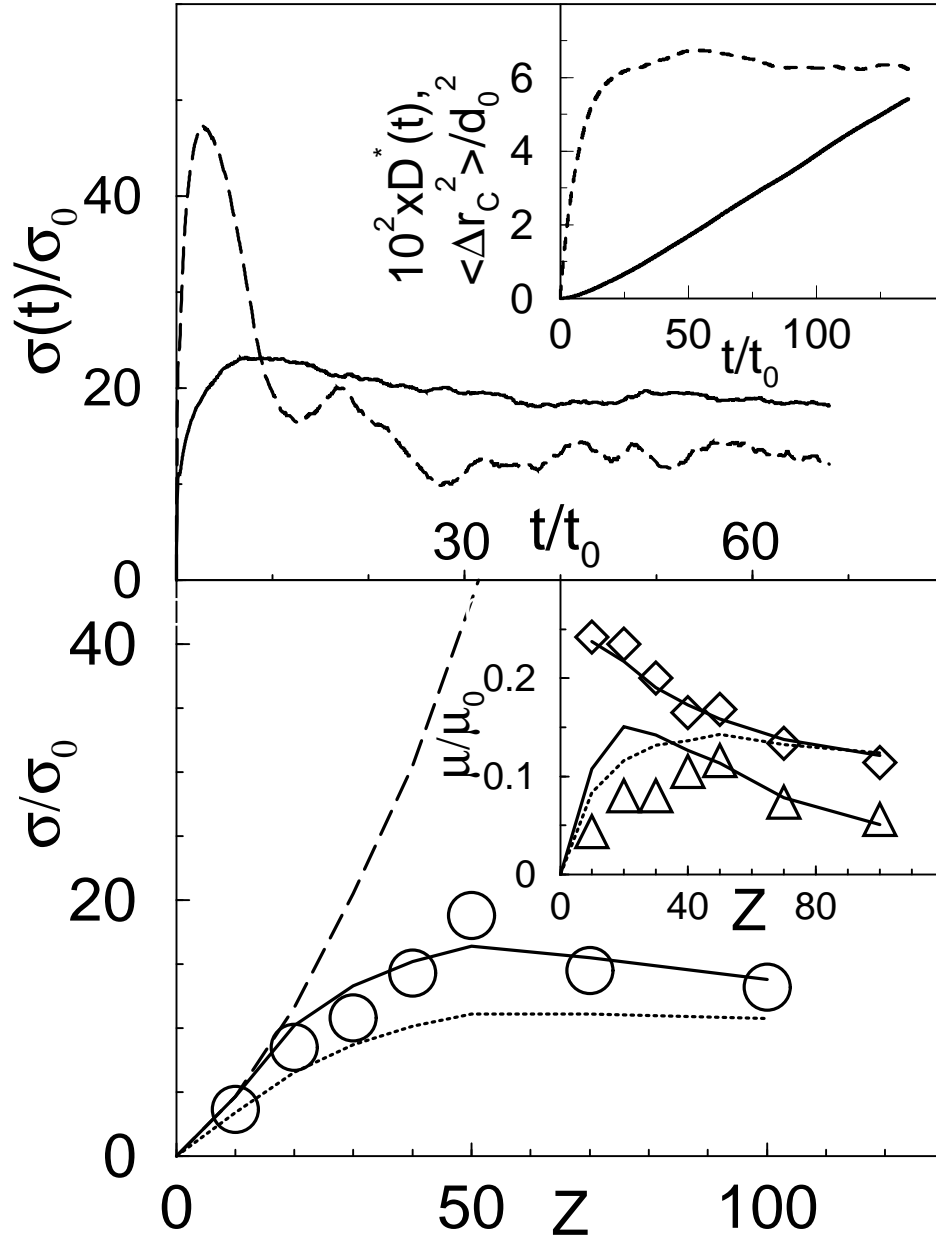


FIG. 3: Top: time-dependent electrical conductivity for $Z = 50$ (solid line) and $Z = 100$ (dashed line); inset: time-dependent diffusion coefficient (dashed line) and mean-squared displacement (solid line) for colloidal particles with $Z = 50$. Bottom: electrical conductivity - simulations (circles) and Eq. 13 (dashed line), Eq. 15 with $Z_{eff}^* = Z_{eff}$ (dotted line) and Eq. 17 with $Z_{eff}^* = 1.4Z_{eff}$ (solid line). Inset: electrophoretic mobilities (absolute values) of the colloidal particles (triangles) and counterions (diamonds - shifted up 0.1 units); solid lines are Eqs. 18 and dotted line is $eZ_{eff}D_C/k_BT$.

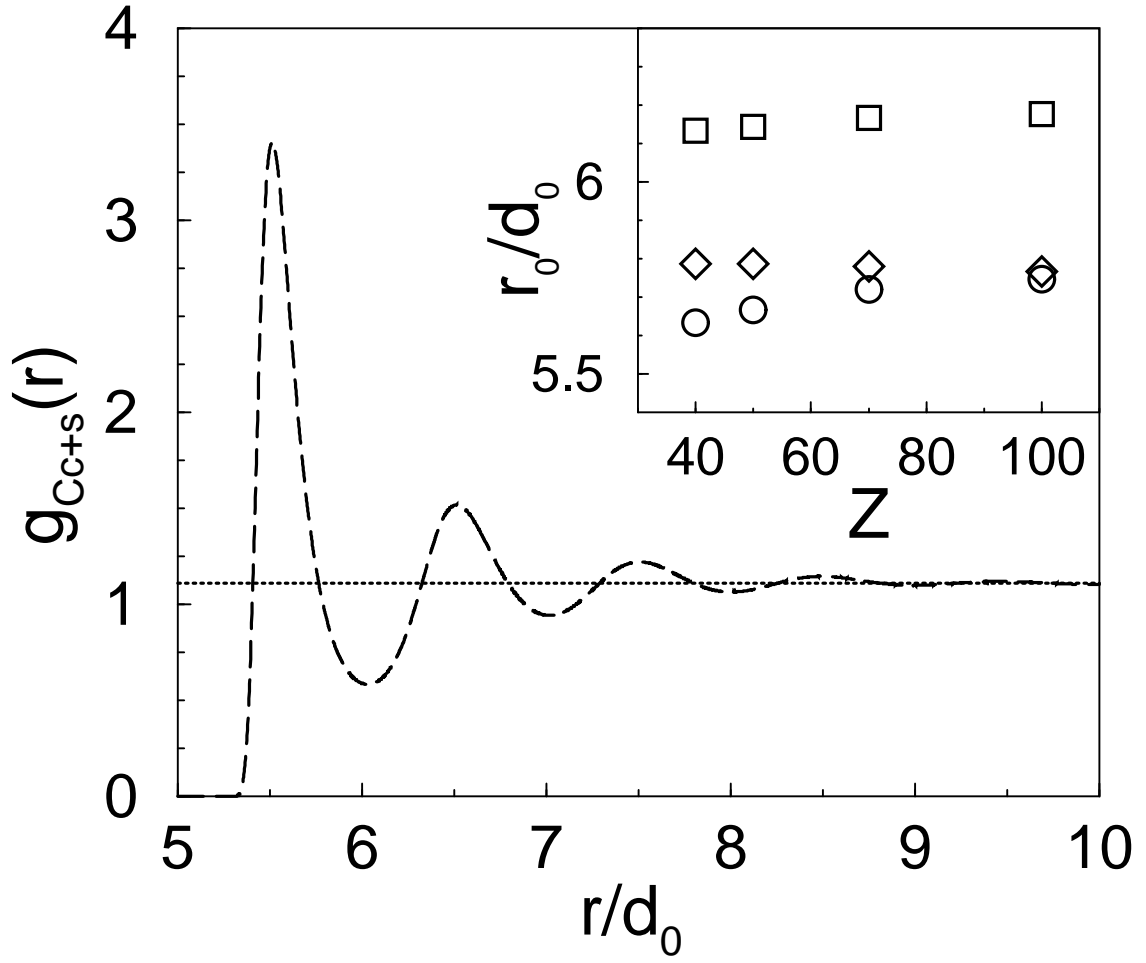


FIG. 4: Colloid-(solvent+counterions) pair correlation function $g_{Cc+s}(r)$ - dashed line; dotted line corresponds to $1/(1 - \phi_C)$. Inset: first minimum of $g_{Cc}(r)$ - r_0 (squares), fluid layer boundary - r_b (see text) (diamonds), and charge shell boundary corresponding to $1.4Z_{eff} - r_\sigma$ (circles).